

Dynamical facilitation governs glassy dynamics in suspensions of colloidal ellipsoids

Chandan K. Mishra^a, K. Hima Nagamanasa^a, Rajesh Ganapathy^b, A. K. Sood^{b,c}, and Shreyas Gokhale^{c,1}

^aChemistry and Physics of Materials Unit and ^bInternational Centre for Materials Science, Jawaharlal Nehru Centre for Advanced Scientific Research, Jakkur, Bangalore 560064, India; and ^cDepartment of Physics, Indian Institute of Science, Bangalore 560012, India

Edited by David Chandler, University of California, Berkeley, CA, and approved September 15, 2014 (received for review July 16, 2014)

One of the greatest challenges in contemporary condensed matter physics is to ascertain whether the formation of glasses from liquids is fundamentally thermodynamic or dynamic in origin. Although the thermodynamic paradigm has dominated theoretical research for decades, the purely kinetic perspective of the dynamical facilitation (DF) theory has attained prominence in recent times. In particular, recent experiments and simulations have highlighted the importance of facilitation using simple model systems composed of spherical particles. However, an overwhelming majority of liquids possess anisotropy in particle shape and interactions, and it is therefore imperative to examine facilitation in complex glass formers. Here, we apply the DF theory to systems with orientational degrees of freedom as well as anisotropic attractive interactions. By analyzing data from experiments on colloidal ellipsoids, we show that facilitation plays a pivotal role in translational as well as orientational relaxation. Furthermore, we demonstrate that the introduction of attractive interactions leads to spatial decoupling of translational and rotational facilitation, which subsequently results in the decoupling of dynamical heterogeneities. Most strikingly, the DF theory can predict the existence of reentrant glass transitions based on the statistics of localized dynamical events, called excitations, whose duration is substantially smaller than the structural relaxation time. Our findings pave the way for systematically testing the DF approach in complex glass formers and also establish the significance of facilitation in governing structural relaxation in supercooled liquids.

glass transition | dynamical facilitation | anisotropic colloids

The transformation of liquids into glasses is as ubiquitous as it is enigmatic. From the formation of obsidian during volcanic eruptions (1) and fabrication of superstrong metallic glasses (2) to exotic forms of slow dynamics in crystals of colloidal dimers (3) and Janus particles (4), glass formation pervades nature, industry, and academia. A vast majority of molecular glass-forming materials exhibit anisotropy in shape and interparticle interactions, which often has a profound influence on their glassy dynamics. The rapidly expanding repertoire of chemists has made it possible to design colloidal particles of desired shape and interactions that can serve as realistic experimental analogs of these molecular liquids (5). By contrast, prominent theories like the Adam–Gibbs (6) theory, random first-order transition (RFOT) theory (7, 8), and the dynamical facilitation (DF) theory (9, 10) have been tested predominantly on spherical glass formers with isotropic interactions, which exhibit gross features of glassy dynamics, but fail to capture the nuances of vitrification in complex systems.

The discovery of growing static (11–16) and dynamic (17–21) length scales appears to support the thermodynamic perspective of the Adam–Gibbs and RFOT theories. However, the growth in static length scales over the dynamical range accessible to numerical simulations is often minuscule and much smaller than the corresponding growth in dynamic length scales (21, 22). This renders any causal connection between growing static length scales and growing timescales doubtful (22). Moreover, recent simulations (23) and colloid experiments (24) have shown that growing dynamical correlations in the form of string-like cooperative motion emerge naturally within the purely kinetic

approach of the DF theory. To compound matters further, facilitation is present even within the RFOT framework, albeit as a consequence of slow dynamics rather than a cause (25). Thus, although DF has been shown to exist (23, 24, 26–29), its relative importance as a mechanism of structural relaxation is still debated (30–32). The application of the DF approach to complex glass formers will therefore not only enhance our understanding of glass transitions in these systems, but also help ascertain the relevance of facilitation in governing structural relaxation.

Here, we apply the DF theory to elucidate glass formation in suspensions of colloidal ellipsoids with repulsive as well as attractive interactions. The DF theory claims that structural relaxation in glass-forming liquids proceeds via a process known as dynamical facilitation, whereby localized mobile regions, termed excitations, mediate motion in neighboring regions in a manner that conserves mobility (9, 10). We first show that the notions of localized excitations and facilitated dynamics can be extended even to orientational relaxation. Next, we demonstrate that the spatial decoupling of dynamical heterogeneities (DHs) observed in colloid experiments stems from the spatial decoupling of rotational and translational facilitation. Most importantly, the DF theory can predict the existence of recently observed reentrant glass transitions (33) from the density dependence of the concentration of excitations. Our findings not only highlight the importance of facilitated dynamics in anisotropic glass formers but also reinforce the claim that, in the broader context of the glass transition, facilitation dominates structural relaxation.

Results and Discussion

Facilitated Dynamics of Rotational and Translational Excitations. We analyzed data from video microscopy experiments (33) on

Significance

Although glasses have been used for a plethora of applications since times immemorial, the basic physics underlying their formation remains mysterious. Furthermore, although competing theories are routinely tested in glass formers comprising spherical particles, little is known about anisotropic systems, despite the fact that most molecular liquids exhibit anisotropy in shape and interactions. Here, we have applied the dynamical facilitation (DF) approach, a prominent theory of the glass transition, to study glass formation in suspensions of colloidal ellipsoids with attractive interactions. We observe that DF can not only explain the phenomenology of glass formation in ellipsoids but also predict the existence of reentrant glass transitions, suggesting that DF can be the dominant mechanism of structural relaxation in realistic glass formers.

Author contributions: C.K.M., K.H.N., R.G., A.K.S., and S.G. designed research; C.K.M. performed research; S.G. contributed new reagents/analytic tools; K.H.N. and S.G. analyzed data; and C.K.M., K.H.N., R.G., A.K.S., and S.G. wrote the paper.

The authors declare no conflict of interest.

This article is a PNAS Direct Submission.

¹To whom correspondence should be addressed. Email: gokhale@physics.iisc.ernet.in.

This article contains supporting information online at www.pnas.org/lookup/suppl/doi:10.1073/pnas.1413384111/-DCSupplemental.

quasi-2D monolayers of colloidal polystyrene ellipsoids of aspect ratio $\alpha=2.1$, with semimajor axis $l=2.1 \mu\text{m}$ and semi-minor axis $w=1 \mu\text{m}$ (*Materials and Methods*). We first identified translational and rotational excitations for ellipsoids with purely repulsive interactions by following the prescription of ref. 23. Accordingly, a particle was said to be associated with a translational (rotational) excitation of size a_r (a_θ) and “instanton” time Δt_r (Δt_θ), if it underwent a linear (angular) displacement of magnitude a_r (a_θ) over a time interval Δt_r (Δt_θ), and persisted in its initial and final positions for at least as long as the instanton time duration. To identify excitations, we first generated coarse-grained translational and rotational trajectories, $\bar{\mathbf{r}}_i(t)$ and $\bar{\theta}_i(t)$, respectively, for every particle i , and computed the functionals:

$$h_i^r(t, t_r; a_r) = \prod_{t'=t_r/2-\Delta t_r}^{t_r/2} \mathcal{H}(|\bar{\mathbf{r}}_i(t+t') - \bar{\mathbf{r}}_i(t-t')| - a_r) \quad [1]$$

$$h_i^\theta(t, t_\theta; a_\theta) = \prod_{t'=t_\theta/2-\Delta t_\theta}^{t_\theta/2} \mathcal{H}(|\bar{\theta}_i(t+t') - \bar{\theta}_i(t-t')| - a_\theta).$$

Here, $\mathcal{H}(x)$ is the Heaviside step function, and t_r and t_θ are “commitment” times that are typically chosen to be approximately three to four times the respective mean instanton times (24) (see *SI Text* for details). In this work, we varied a_r and a_θ in the range $0.33l \leq a_r \leq 0.83l$ and $10^\circ \leq a_\theta \leq 25^\circ$, respectively. We note that a_r and a_θ are characteristics of translational and rotation excitations, respectively, and are independent of the thermodynamic state of the system. Instead, it is the concentration of these excitations that is expected to decrease on approaching the glass transition (23, 24). We observe that, analogous to spherical colloids (24), the distributions of instanton times for translational [$P_r(\Delta t_r)$] as well as rotational [$P_\theta(\Delta t_\theta)$] excitations remain fairly localized for all area fractions ϕ (Fig. 1 A and B). Furthermore, the peak instanton times Δt_r^p and Δt_θ^p do not grow with ϕ and are much smaller than the corresponding structural relaxation times τ_α at large ϕ (33). Thus, rotational excitations cannot only be defined using the procedure developed in ref. 23, but are also temporally localized, as postulated by the DF theory.

Next, we quantified the spatial extent of rotational and translational excitations, by computing the functions:

$$\mu_{rr}(r, t, t'; a_r) = \frac{1}{\rho \mu_\infty^r(t'-t) \langle h_1^r(0, t_r; a_r) \rangle} \left\langle h_1^r(0, t_r; a_r) \times \sum_{i \neq 1}^N |\bar{\mathbf{r}}_i(t') - \bar{\mathbf{r}}_i(t)| \delta(|\bar{\mathbf{r}}_i(t) - \bar{\mathbf{r}}_1(t) - r|) \right\rangle \quad [2]$$

$$\mu_{\theta\theta}(r, t, t'; a_\theta) = \frac{1}{\rho \mu_\infty^\theta(t'-t) \langle h_1^\theta(0, t_\theta; a_\theta) \rangle} \left\langle h_1^\theta(0, t_\theta; a_\theta) \times \sum_{i \neq 1}^N |\bar{\theta}_i(t') - \bar{\theta}_i(t)| \delta(|\bar{\mathbf{r}}_i(t) - \bar{\mathbf{r}}_1(t) - r|) \right\rangle.$$

Here, ρ is the particle number density, $\mu_\infty^r(t) = \langle |\bar{\mathbf{r}}_i(t) - \bar{\mathbf{r}}_i(0)| \rangle$, $\mu_\infty^\theta(t) = \langle |\bar{\theta}_i(t) - \bar{\theta}_i(0)| \rangle$, and the angular brackets indicate averaging over time. The functions $\mu_{rr}(r, -t_r/2, t_r/2; a_r)$ and $\mu_{\theta\theta}(r, -t_\theta/2, t_\theta/2; a_\theta)$, respectively, yield the translational and rotational displacement density at a distance r from a translational or rotational excitation of a given size centered at the origin at time $t=0$, over the corresponding commitment times t_r and t_θ . We observed that for all ϕ , $\mu_{rr}(r, -t_r/2, t_r/2; a_r)$ and $\mu_{\theta\theta}(r, -t_\theta/2, t_\theta/2; a_\theta)$ stabilize at 1 within $6-8l$ (Fig. 1 C and D), confirming that in accordance with the DF theory, rotational as well as translational excitations are spatially localized

objects that do not exhibit any growth as the glass transition is approached.

One of the two central tenets of the DF theory is a decrease in the concentration of excitations on approaching the glass transition. This concentration can be visualized from the normalized translational and rotational displacement fields $|\Delta \mathbf{r}_i(t_r)|/a_r$ and $|\Delta \theta_i(t_\theta)|/a_\theta$, respectively. Fig. 1 E and F shows these displacement fields for $\phi=0.73$ and $\phi=0.79$. In Fig. 1E, the maroon regions denote particles that undergo displacements larger than the excitation size $a_r=0.33l$ over the corresponding commitment time t_r , and therefore indicate the presence of translational excitations. Similarly, the maroon regions in Fig. 1F denote

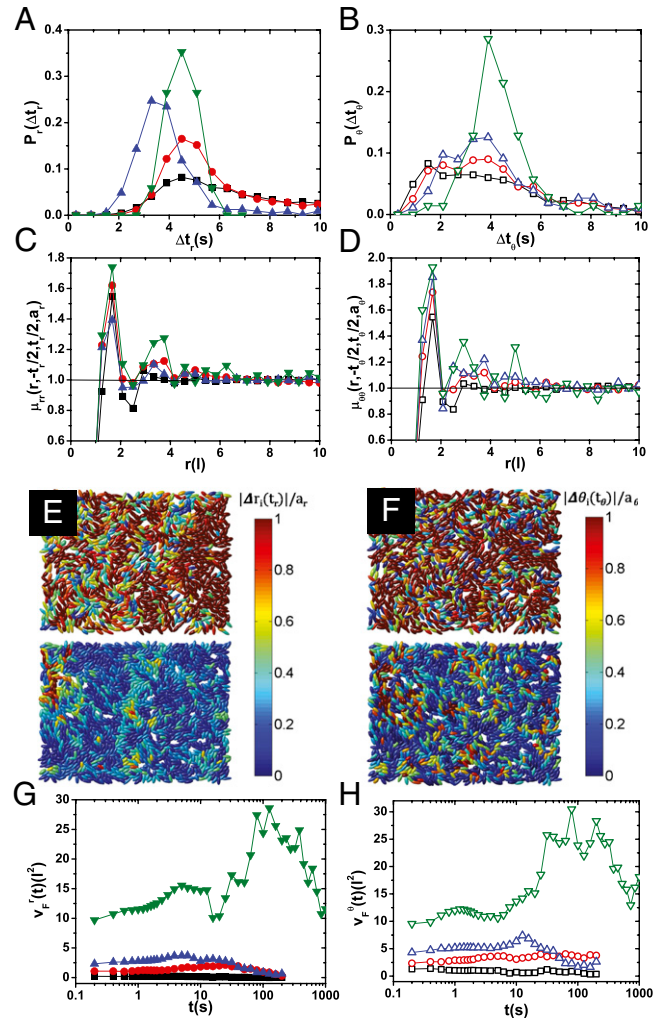


Fig. 1. Facilitation in translational and orientational degrees of freedom. (A) Instanton time distribution $P_r(\Delta t_r)$ for translational excitations of size $a_r = 0.33l$ for $\phi = 0.68$ (■), $\phi = 0.73$ (●), $\phi = 0.76$ (▲), and $\phi = 0.79$ (▼). (B) Instanton time distribution $P_\theta(\Delta t_\theta)$ for rotational excitations of size $a_\theta = 10^\circ$ for $\phi = 0.68$ (□), $\phi = 0.73$ (○), $\phi = 0.76$ (△), and $\phi = 0.79$ (▽). (C) The function $\mu_{rr}(r, -t_r/2, t_r/2; a_r)$ for $a_r = 0.33l$ for various ϕ . The colors and symbols are identical to those in A. (D) The function $\mu_{\theta\theta}(r, -t_\theta/2, t_\theta/2; a_\theta)$ for $a_\theta = 10^\circ$ for various ϕ . The colors and symbols are identical to those in B. (E) The translational displacement field $|\Delta \mathbf{r}_i(t_r)|$ normalized by $a_r = 0.33l$. (F) The rotational displacement field $|\Delta \theta_i(t_\theta)|$ normalized by $a_\theta = 10^\circ$. In E and F, the top panels correspond to $\phi = 0.73$, and the bottom panels correspond to $\phi = 0.79$. (G) Facilitation volume for translational excitations, $v_r^p(t)$, for $a_r = 0.33l$ for various ϕ . The colors and symbols are identical to those in A. (H) Facilitation volume for rotational excitations, $v_\theta^p(t)$, for $a_\theta = 10^\circ$ for various ϕ . The colors and symbols are identical to those in B.

particles that undergo angular displacements larger than $a_\theta = 10^\circ$ over t_θ , thus serving as an indicator of the concentration of rotational excitations. It is obvious from Fig. 1 E and F that the concentration of translational as well as rotational excitations indeed decreases with ϕ , in concord with the DF theory. The concentration of translational excitations, c_r , and rotational excitations, c_θ , can be formally defined as follows:

$$c_r = \left\langle \frac{1}{Vt_r} \sum_{i=1}^N h_i^r(0, t_r; a_r) \right\rangle$$

$$c_\theta = \left\langle \frac{1}{Vt_\theta} \sum_{i=1}^N h_i^\theta(0, t_\theta; a_\theta) \right\rangle, \quad [3]$$

where V is the volume, N is the total number of particles, and the angular brackets indicate averaging over time. c_r and c_θ play an especially important role in the prediction of reentrant glass transitions in translational and rotational degrees of freedom.

The second major claim of the DF theory is that mobility cannot be spontaneously created or destroyed, and hence excitations, which are carriers of mobility, must always occur in the vicinity of existing excitations. From the functions defined in Eq. 2, we extracted facilitation volumes, which serve as measures of facilitated dynamics in translational as well as rotational degrees of freedom:

$$v_F^r(t) = \int \left[\frac{\mu_{rr}(r, t_r/2, t; a_r)}{g(r)} - 1 \right] d\mathbf{r}$$

$$v_F^\theta(t) = \int \left[\frac{\mu_{\theta\theta}(r, t_\theta/2, t; a_\theta)}{g(r)} - 1 \right] d\mathbf{r}. \quad [4]$$

Here, $g(r)$ is the radial pair correlation function. These facilitation volumes quantify the size of the region around an excitation in which structural relaxation at time t can be unambiguously attributed to the presence of the initial excitation. We note that, because our system is 2D, $v_F^r(t)$ and $v_F^\theta(t)$ are actually areas, although we shall henceforth refer to them as facilitation volumes to allow comparison with prior work (23, 24). We observe once again that, in close analogy with colloidal spheres (24), the profiles of $v_F^r(t)$ as well as $v_F^\theta(t)$ generically exhibit a maximum (Fig. 1 G and H). In general, facilitation volumes depend on the concentration of excitations, which in turn depends on the excitation size (23). Here, we have chosen a_r and a_θ such that the peak instanton times for translational and rotational excitations are comparable, i.e., $\Delta t_p^r \sim \Delta t_p^\theta$ (Fig. 1 A and B), a fact that is also reflected in the facilitation volumes (Fig. 1 G and H). Furthermore, we see the maximum values $v_F^r(t)$ and $v_F^\theta(t)$ as well as the time taken to reach the maximum increase with ϕ , showing that facilitated dynamics becomes increasingly apparent on approaching the glass transition (23, 34), even in systems with orientational degrees of freedom (see [Movies S1](#) and [S2](#) for a visualization of facilitated dynamics in translational and rotational degrees of freedom, respectively).

Coupling Between Rotational and Translational Facilitation. Because excitations are, by definition, carriers of mobility, it is natural to identify them from particle displacements in systems with purely translational degrees of freedom, such as those in refs. 23 and 24. In ellipsoids, however, mobility is distributed between particle translations and rotations, and hence, facilitation in the two degrees of freedom does not occur independently. In particular, translational excitations can facilitate rotational relaxation and vice versa. To quantify this coupling in translational and rotational facilitation, we defined mixed variants of the functions in Eq. 2:

$$\mu_{r\theta}(r, t, t'; a_r) = \frac{1}{\rho\mu_\infty^\theta(t-t)} \left\langle h_1^r(0, t_r; a_r) \right.$$

$$\left. \times \sum_{i \neq 1}^N |\bar{\theta}_i(t') - \bar{\theta}_i(t)| \delta(|\bar{\mathbf{r}}_i(t) - \bar{\mathbf{r}}_1(t)| - r) \right\rangle$$

$$\mu_{\theta r}(r, t, t'; a_\theta) = \frac{1}{\rho\mu_\infty^r(t-t)} \left\langle h_1^\theta(0, t_\theta; a_\theta) \right.$$

$$\left. \times \sum_{i \neq 1}^N |\bar{\mathbf{r}}_i(t') - \bar{\mathbf{r}}_i(t)| \delta(|\bar{\mathbf{r}}_i(t) - \bar{\mathbf{r}}_1(t)| - r) \right\rangle. \quad [5]$$

The mixed, or “off-diagonal” functions $\mu_{r\theta}(r, t, t'; a_r)$ and $\mu_{\theta r}(r, t, t'; a_\theta)$ exhibit qualitatively similar behavior to their pure, or “diagonal” counterparts (Fig. 2A). Interestingly, we see that the first peak of $\mu_{r\theta}(r, t, t'; a_r)$ is sharper than that of $\mu_{\theta r}(r, t, t'; a_\theta)$, which suggests that the influence of translational excitations on rotational dynamics is stronger than that of rotational excitations on translational dynamics. To investigate whether this imbalance in facilitation is a generic feature of our system, we calculated the asymmetry parameter $F(a_r, a_\theta, t_m) = \mu_{r\theta}^{\max}(t_m)/\mu_{\theta r}^{\max}(t_m)$ for 16 different combinations of a_r and a_θ for $\phi = 0.73$. Here, $\mu_{r\theta}^{\max}(t_m)$ and $\mu_{\theta r}^{\max}(t_m)$ are the first maxima of $\mu_{r\theta}(r, -t_m/2, t_m/2; a_r)$ and $\mu_{\theta r}(r, -t_m/2, t_m/2; a_\theta)$, respectively, and $t_m = \max(t_r, t_\theta)$. We find that $F(a_r, a_\theta, t_m)$ is greater than 1 for 14 of the 16 combinations of a_r and a_θ considered (Fig. 2B). For the remaining two combinations, we find that $\Delta t_p^\theta > \Delta t_p^r$, suggesting that the low values of $F(a_r, a_\theta, t_m)$ in these cases stem from the disparity in the sizes of rotational and translational excitations. For cases in which $\Delta t_p^r \sim \Delta t_p^\theta$, $F(a_r, a_\theta, t_m) \sim 1.2$, which shows that the impact of translational excitations on rotational relaxation is indeed more profound compared with that of rotational ones on translational relaxation. From the nature of collisions in a dense, orientationally and translationally disordered system, one would expect a large translation of a particle to induce large rotations in its vicinity in addition to inducing translations. Further large rotational motions would be likelier to induce rotational rather than translational motion in the particle’s neighborhood. The observed asymmetry in facilitated dynamics is consistent with this intuitive picture. Next, we computed the corresponding off-diagonal facilitation volumes $v_F^{r\theta}(t)$ and $v_F^{\theta r}(t)$, defined analogously to Eq. 4 (Fig. S1), and found that the maximum of $v_F^{r\theta}(t)$ increases more rapidly with ϕ compared with that of $v_F^{\theta r}(t)$ (Fig. 2C). This implies that the asymmetry in facilitation becomes increasingly pronounced on approaching the glass transition.

Spatial Decoupling of DHs and Prediction of Reentrant Glass Transitions. Having elucidated the nature of facilitated dynamics in the case of ellipsoids with short-ranged repulsions, we turn our attention to the influence of attractive depletion interactions on glass formation. Depletion interactions between particles are known to depend on local curvature (35, 36). For ellipsoids, therefore, these interactions are anisotropic and favor the alignment of particles along their major axis (33). We first examine the effect of attractive interactions on the spatial coupling between translational and rotational facilitation. From the height of the first peak of the functions defined in Eqs. 2 and 5, we computed the facilitation coupling coefficient:

$$C_F(a_r, a_\theta, t_m) = \frac{\mu_{r\theta}^{\max}(t_m)\mu_{\theta r}^{\max}(t_m)}{\mu_{rr}^{\max}(t_m)\mu_{\theta\theta}^{\max}(t_m)}. \quad [6]$$

Here, in analogy to $\mu_{r\theta}^{\max}(t_m)$ and $\mu_{\theta r}^{\max}(t_m)$, $\mu_{rr}^{\max}(t_m)$ and $\mu_{\theta\theta}^{\max}(t_m)$ are the first maxima of $\mu_{rr}(r, -t_m/2, t_m/2; a_r)$ and $\mu_{\theta\theta}(r, -t_m/2, t_m/2; a_\theta)$, respectively, and once again, $t_m = \max(t_r, t_\theta)$. $C_F(a_r, a_\theta, t_m)$ is greater than 1 if excitations in one degree of freedom have a greater influence on relaxation in

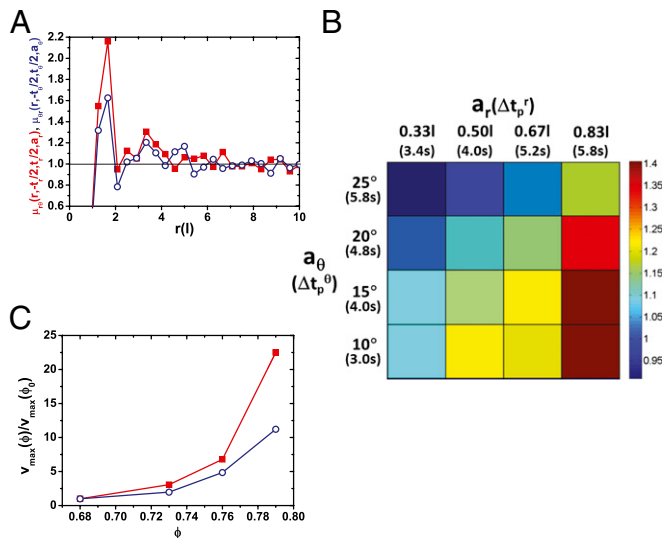


Fig. 2. Coupling between translational and rotational facilitation. (A) The off-diagonal functions $\mu_{r0}(r, -t_r/2, t_r/2; a_r)$ (red \blacksquare) and $\mu_{\theta r}(r, -t_\theta/2, t_\theta/2; a_\theta)$ (blue \circ) for $\phi = 0.76$. The values $a_r = 0.51$ and $a_\theta = 15^\circ$ are chosen such that $\Delta t_r^t \sim \Delta t_\theta^t$. (B) Facilitation volume profiles for the off-diagonal functions in C. (C) The asymmetry parameter $F(a_r, a_\theta, t_m)$ for various combinations of a_r and a_θ . The corresponding values of Δt_r^t and Δt_θ^t are enclosed in parentheses. The colorbar corresponds to the values of $F(a_r, a_\theta, t_m)$. (D) The maxima of the off-diagonal facilitation volumes, v_{\max}^r and v_{\max}^θ as a function of ϕ , normalized by their respective values at $\phi_0 = 0.68$. The colors and symbols are identical to those in A.

the other degree of freedom compared with the same one. We see that $C_F(a_r, a_\theta, t_m)$ is lower for $\Delta U/k_B T = 1.16$ compared with the repulsive case ($\Delta U/k_B T = 0$), and increases upon further increasing $\Delta U/k_B T$, especially at large ϕ (Fig. 3A). Next, we examined the rotational and translational contributions to $C_F(a_r, a_\theta, t_m)$ separately, by defining the coefficients $C_F^r = \mu_{r0}^{\max} / \mu_{\theta r}^{\max}$ and $C_F^\theta = \mu_{\theta r}^{\max} / \mu_{r0}^{\max}$. We observe that C_F^r varies little across ϕ as well as $\Delta U/k_B T$, and the behavior of $C_F(a_r, a_\theta, t_m)$ is dominated by C_F^θ (Fig. 3B). This reinforces the finding of Fig. 2 that translational excitations play a more crucial role in rotational relaxation than vice versa.

It has been shown in simulations (23) as well as experiments (24) that the hierarchical facilitated dynamics of excitations culminates in string-like cooperative motion (17), and in particular, excitations are analogous to “microstrings” (37). It is therefore tempting to wonder whether growing dynamic correlations generically emerge from excitation dynamics. If this is indeed the case, the spatial decoupling of rotational and translational facilitation in our system should lead to a decoupling of DHs in the two degrees of freedom. To investigate this possibility, we defined a coupling coefficient for DH by identifying the top 10% of the translationally and rotationally most mobile particles over a time interval Δt . We first computed the distribution $P(r, \Delta t)$ of the minimum distance between each translationally mobile particle and the set of rotationally mobile particles. We also computed a reference distribution $P^*(r, \Delta t)$ of the minimum distance of translationally mobile particles from a set of randomly chosen nonmobile particles. We then computed the coupling function:

$$D(\Delta t) = \frac{\int_0^{r_{\min}} P(r, \Delta t) dr}{\int_0^{r_{\min}} P^*(r, \Delta t) dr}, \quad [7]$$

where r_{\min} is the first minimum of the radial pair correlation function. $D(\Delta t)$ is analogous to the mobility transfer function defined in ref. 26, except that instead of considering translationally mobile particles in two subsequent intervals, we consider

translationally and rotationally mobile particles in the same interval. We observe that for all ϕ s (Fig. 3C) and depletion interaction strengths $\Delta U/k_B T$ considered (Fig. S2), $D(\Delta t)$ shows a peak around $\Delta t \sim t^*$, where t^* is the cage-breaking time, i.e., the time at which the non-Gaussian parameter $\alpha_2(t)$ reaches a maximum. We chose the maximum value of $D(\Delta t)$, D_{\max} , as the coupling coefficient for DH. We observe that for all $\Delta U/k_B T$, D_{\max} increases with ϕ , which indicates that the spatial coupling between rotational and translational DH increases on approaching the glass transition (Fig. 3D). More interestingly, in striking resemblance with the behavior of $C_F(a_r, a_\theta, t_m)$ (Fig. 3A), we find that for $\Delta U/k_B T = 1.16$, D_{\max} is lower than the purely repulsive case (Fig. 3D). On increasing $\Delta U/k_B T$ further, we see that D_{\max} once again begins to increase, which is consistent with the dependence of $C_F(a_r, a_\theta, t_m)$ on $\Delta U/k_B T$ (Fig. 3A). These findings show that the spatial decoupling of facilitated dynamics indeed results in the spatial decoupling of rotational and translational DH.

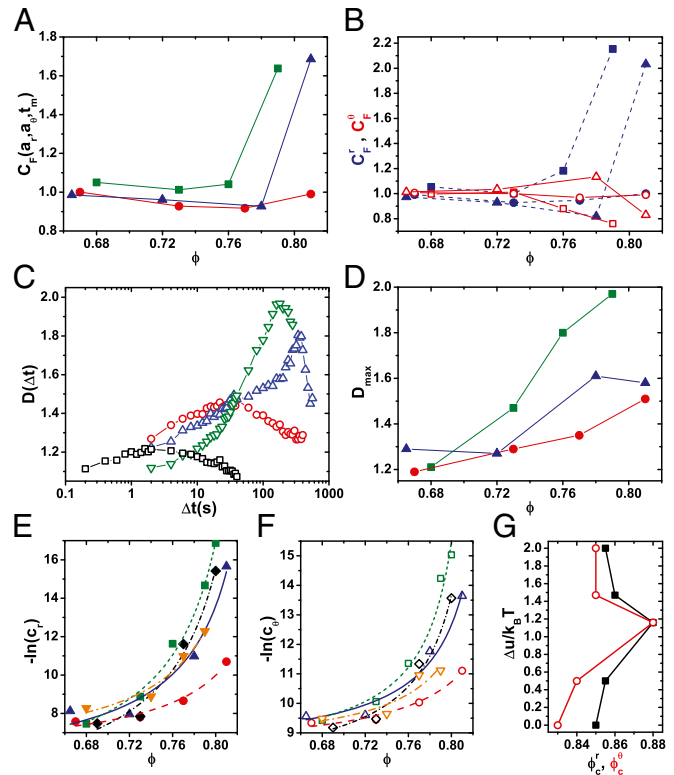


Fig. 3. Spatial decoupling of heterogeneities and prediction of reentrant glass transitions. (A) The coupling coefficient for facilitation, $C_F(a_r, a_\theta, t_m)$, with $a_r = 0.51$ and $a_\theta = 20^\circ$, as a function of ϕ for $\Delta U/k_B T = 0$ (green \blacksquare), $\Delta U/k_B T = 1.16$ (red \bullet), and $\Delta U/k_B T = 1.47$ (blue \blacktriangle). (B) The translational and rotational contributions to $C_F(a_r, a_\theta, t_m)$, C_F^r (filled blue symbols), and C_F^θ (hollow red symbols), respectively, as a function of ϕ for $\Delta U/k_B T = 0$ (squares), $\Delta U/k_B T = 1.16$ (circles), and $\Delta U/k_B T = 1.47$ (triangles). (C) The coupling function for DHs, $D(\Delta t)$, in the purely repulsive case, $\Delta U/k_B T = 0$, for $\phi = 0.68$ (\square), $\phi = 0.73$ (red \circ), $\phi = 0.76$ (blue \triangle), and $\phi = 0.79$ (green ∇). (D) The coupling coefficient for DHs, D_{\max} , as a function of ϕ for $\Delta U/k_B T = 0$ (green \blacksquare), $\Delta U/k_B T = 1.16$ (red \bullet), and $\Delta U/k_B T = 1.47$ (blue \blacktriangle). (E) The ϕ dependence of the concentration of translational excitations c_r for $a_r = 0.51$, for $\Delta U/k_B T = 0$ (green \blacksquare), $\Delta U/k_B T = 0.47$ (\blacklozenge), $\Delta U/k_B T = 1.16$ (red \bullet), $\Delta U/k_B T = 1.47$ (blue \blacktriangle), and $\Delta U/k_B T = 1.95$ (yellow \blacktriangledown). (F) The ϕ dependence of the concentration of rotational excitations c_θ for $a_\theta = 20^\circ$ for $\Delta U/k_B T = 0$ (green \square), $\Delta U/k_B T = 0.47$ (\diamond), $\Delta U/k_B T = 1.16$ (red \circ), $\Delta U/k_B T = 1.47$ (blue \triangle), and $\Delta U/k_B T = 1.95$ (yellow ∇). In E and F, the concentrations c_r and c_θ , respectively, are reported in units of l^2 -seconds $^{-1}$. The curves are empirical fits of the form $\phi_0 + A(\phi_c - \phi)^{-1}$. (G) The translational glass transition ϕ_c^r (\blacksquare) and rotational glass transition ϕ_c^θ (red \circ) obtained from fits to the curves in E and F, for various values of $\Delta U/k_B T$.

Having established the close link between facilitation and DH in rotational as well as translational dynamics, we examine in the influence of attractive interactions on the concentration of translational and rotational excitations c_r and c_θ , respectively (Eq. 3). Within the DF theory, the concentration of excitations must vanish at the glass transition. The ϕ dependence of c_r and c_θ can therefore provide valuable information on the location of glass transitions in our system. Fig. 3E shows the ϕ dependence of the concentration of translational excitations, c_r , for three different strengths of the attractive interaction $\Delta U/k_B T$. We see that for $\Delta U/k_B T = 0$, $-\ln(c_r)$ appears to diverge at some $\phi = \phi_c^t$, which we identify as the translational glass transition. Interestingly, with increasing attraction, ϕ_c^t first shifts to a larger value for $\Delta U/k_B T = 1.16$, and then decreases upon further increasing $\Delta U/k_B T$ to 1.47. Similar qualitative behavior is also exhibited by the orientational glass transition area fraction ϕ_c^θ (Fig. 3F). Furthermore, we observe that this trend is robust and persists for different values of a_r and a_θ (Fig. S3). This shows that the presence of attractive interactions induces reentrant glass transitions in translational as well as orientational degrees of freedom (Fig. 3G). The presence of reentrant glass transitions in this system was previously inferred (33) from the mode coupling theory (MCT) scaling of relaxation times (38, 39). However, we emphasize that the prediction of the DF theory is based on the statistics of localized dynamical events that occur on timescales far smaller than the structural relaxation time. Furthermore, we note that the ϕ_c^t and ϕ_c^θ values obtained from the MCT scaling analysis (33) are smaller than the corresponding values obtained here (Fig. 3G). This is possibly a reflection of the fact that the MCT scaling yields the laboratory glass transition at $\phi = \phi_g$, whereas the concentration of excitations yields the jamming transition at $\phi = \phi_j$. Also, it must be noted that, although the empirical fitting procedure used to extract ϕ_c^t and ϕ_c^θ is useful to illustrate the reentrance in glass transitions, an analysis of the shapes of the glass transition lines would require far more rigorous theoretical treatment. As a final remark, we note that the observed shift in ϕ_c^t and ϕ_c^θ with $\Delta U/k_B T$ is qualitatively consistent with the spatial decoupling of facilitated dynamics as well as DHs. Because $C_F(a_r, a_\theta, t_m)$ and D_{max} increase with ϕ (Fig. 3A and D), they are indicators of the system's proximity to the glass transition. The addition of attractive interaction lowers both $C_F(a_r, a_\theta, t_m)$ and D_{max} for a given ϕ . This indicates that the system moves further away from the glass transition on introducing attractions, which in turn implies that the glass transition shifts to larger ϕ , as seen in Fig. 3G.

Conclusions

In summary, we have expanded the concepts of localized excitations and facilitated dynamics to include systems with orientational degrees of freedom (Fig. 1). By applying this extended framework of DF to experimental data on suspensions of colloidal ellipsoids, we have shown that translational excitations have a more pronounced influence on orientational dynamics than vice versa (Fig. 2). Furthermore, we observe that the spatial decoupling of translational and rotational DHs is a consequence of the spatial decoupling of facilitation in these two degrees of freedom (Fig. 3A and D). Most importantly, our results show that the reentrance in translational as well as orientational glass transitions with increasing $\Delta U/k_B T$ (Fig. 3G) can be predicted from the ϕ dependence of the concentration of excitations, sans

prior knowledge of relaxation times (Fig. 3E and F). Collectively, these findings show that dynamical facilitation plays a crucial role in governing structural relaxation even in systems with orientational degrees of freedom. In a broader context, the predictive capability of the facilitation approach demonstrated here strongly suggests that a one-to-one correspondence between the concentration of excitations and the relaxation time, as envisioned in the DF theory, may indeed exist. Our findings immediately open the door for testing the postulates of the DF theory in a variety of complex colloidal systems (5). In particular, it would be instructive to see whether the splitting of rotational and translational glass transitions for ellipsoids with large aspect ratio (40–42) can be explained within the context of facilitation. On the theoretical front, it would be fascinating to examine whether the hierarchy of excitation energies that scale logarithmically with excitation size (23) also exists for orientational degrees of freedom. Furthermore, it would be interesting to see whether the concentration of rotational excitations can yield quantitative predictions for the temperature as well as density dependence of the orientational relaxation time. Another promising avenue is the search for potential connections between structural order and facilitation. In the context of ellipsoids, a link between local order and DHs has already been forged (33, 43). Given the connection between DF and heterogeneities observed here, it would be worthwhile to explore whether the spatial occurrence of excitations is itself dictated by local order. We expect our findings to spur further experimental and theoretical research aimed at answering these questions and thereby serve as a stepping stone to a complete understanding of the glass transition.

Materials and Methods

Details of the materials and methods have been described in ref. 33. Briefly, colloidal polystyrene ellipsoids with major axis $2l = 2.1 \mu\text{m}$ and minor axis $2w = 1 \mu\text{m}$ were synthesized using the method prescribed in ref. 44. The polydispersities in the major and minor axes are 11% and 8%, respectively. Depletion interactions were introduced by adding the nonadsorbing polymer sodium carboxyl methyl cellulose (NaCMC) (Fisher Scientific; M_w , 700,000; r_g , 60 nm). Samples were loaded in wedge-shaped cells and the area fraction ϕ was tuned by controlled sedimentation of the ellipsoids to a monolayer-thick region of cells. The plane containing the axes of the ellipsoids was parallel to the walls of the cell. For every value of $\Delta U/k_B T$, typically 9–10 different cells were examined and the one with the least number of stuck particles was chosen for collecting data. Furthermore, within the chosen cell, several fields of view were scanned to ensure that the region of interest did not contain any stuck particles, and as far as possible, videos for different ϕ were captured within the same region. (See Fig. S4 for representative time-averaged snapshots.) Samples were imaged using a 100 \times oil-immersion objective (Leica; Plan-Apochromat; N.A. 1.4), and videos were captured at a frame rate of 5 frames per s for 20 min. The center of mass coordinates as well as orientations of the ellipsoids were extracted using ImageJ, and trajectories were constructed using standard Matlab particle-tracking algorithms (45). Subsequent analysis was performed using Matlab codes developed in-house.

ACKNOWLEDGMENTS. S.G. thanks the Council for Scientific and Industrial Research (CSIR), India, for a Shyama Prasad Mukherjee Fellowship. K.H.N. thanks CSIR, India, for a Senior Research Fellowship. R.G. thanks the International Centre for Materials Science, Jawaharlal Nehru Centre for Advanced Scientific Research for financial support. A.K.S. thanks Department of Science and Technology, India, for support under J. C. Bose Fellowship.

- Shackley MS (2005) *Obsidian: Geology and Archaeology in the North American Southwest* (Univ of Arizona Press, Tucson, AZ).
- Demetriou MD, et al. (2011) A damage-tolerant glass. *Nat Mater* 10(2):123–128.
- Gerbode SJ, et al. (2010) Glass dislocation dynamics in 2d colloidal dimer crystals. *Phys Rev Lett* 105(7):078301.
- Jiang S, et al. (2014) Orientationally glassy crystals of janus spheres. *Phys Rev Lett* 112(21):218301.
- Glotzer SC, Solomon MJ (2007) Anisotropy of building blocks and their assembly into complex structures. *Nat Mater* 6(8):557–562.
- Adam G, Gibbs JH (1965) On the temperature dependence of cooperative relaxation properties in glass-forming liquids. *J Chem Phys* 43(1):139–146.
- Kirkpatrick T, Thirumalai D, Wolynes PG (1989) Scaling concepts for the dynamics of viscous liquids near an ideal glassy state. *Phys Rev A* 40(2):1045–1054.
- Lubchenko V, Wolynes PG (2007) Theory of structural glasses and supercooled liquids. *Annu Rev Phys Chem* 58:235–266.
- Garrahan JP, Chandler D (2002) Geometrical explanation and scaling of dynamical heterogeneities in glass forming systems. *Phys Rev Lett* 89(3):035704.
- Chandler D, Garrahan J (2010) Dynamics on the way to forming glass: Bubbles in space-time. *Annu Rev Phys Chem* 61:191–217.
- Biroli G, Bouchaud JP, Cavagna A, Grigera T, Verrocchio P (2008) Thermodynamic signature of growing amorphous order in glass-forming liquids. *Nat Phys* 4(10):771–775.

12. Karmakar S, Dasgupta C, Sastry S (2009) Growing length and time scales in glass-forming liquids. *Proc Natl Acad Sci USA* 106(10):3675–3679.
13. Tanaka H, Kawasaki T, Shintani H, Watanabe K (2010) Critical-like behaviour of glass-forming liquids. *Nat Mater* 9(4):324–331.
14. Kurchan J, Levine D (2011) Order in glassy systems. *J Phys A Math Theor* 44(3):035001.
15. Karmakar S, Lerner E, Procaccia I (2012) Direct estimate of the static length-scale accompanying the glass transition. *Physica A* 391(4):1001–1008.
16. Dunleavy AJ, Wiesner K, Royall CP (2012) Using mutual information to measure order in model glass formers. *Phys Rev E Stat Nonlin Soft Matter Phys* 86(4):041505.
17. Donati C, et al. (1998) Stringlike cooperative motion in a supercooled liquid. *Phys Rev Lett* 80(11):2338–2341.
18. Weeks ER, Crocker JC, Levitt AC, Schofield A, Weitz DA (2000) Three-dimensional direct imaging of structural relaxation near the colloidal glass transition. *Science* 287(5453):627–631.
19. Kegel WK, et al. (2000) Direct observation of dynamical heterogeneities in colloidal hard-sphere suspensions. *Science* 287(5451):290–293.
20. Berthier L, et al. (2005) Direct experimental evidence of a growing length scale accompanying the glass transition. *Science* 310(5755):1797–1800.
21. Kob W, Roldán-Vargas S, Berthier L (2012) Non-monotonic temperature evolution of dynamic correlations in glass-forming liquids. *Nat Phys* 8(2):164–167.
22. Charbonneau P, Tarjus G (2013) Decorrelation of the static and dynamic length scales in hard-sphere glass formers. *Phys Rev E Stat Nonlin Soft Matter Phys* 87(4):042305.
23. Keys AS, Hedges LO, Garrahan JP, Glotzer SC, Chandler D (2011) Excitations are localized and relaxation is hierarchical in glass-forming liquids. *Phys Rev X* 1(2):021013.
24. Gokhale S, Nagamanasa KH, Ganapathy R, Sood A (2014) Growing dynamical facilitation on approaching the random pinning colloidal glass transition. *Nat Commun* 5:4685.
25. Bhattacharyya SM, Bagchi B, Wolynes PG (2008) Facilitation, complexity growth, mode coupling, and activated dynamics in supercooled liquids. *Proc Natl Acad Sci USA* 105(42):16077–16082.
26. Vogel M, Glotzer SC (2004) Spatially heterogeneous dynamics and dynamic facilitation in a model of viscous silica. *Phys Rev Lett* 92(25):255901.
27. Bergroth MN, Vogel M, Glotzer SC (2005) Examination of dynamic facilitation in molecular dynamics simulations of glass-forming liquids. *J Phys Chem B* 109(14):6748–6753.
28. Candelier R, Dauchot O, Biroli G (2009) Building blocks of dynamical heterogeneities in dense granular media. *Phys Rev Lett* 102(8):088001.
29. Candelier R, et al. (2010) Spatiotemporal hierarchy of relaxation events, dynamical heterogeneities, and structural reorganization in a supercooled liquid. *Phys Rev Lett* 105(13):135702.
30. Berthier L, Biroli G (2011) Theoretical perspective on the glass transition and amorphous materials. *Rev Mod Phys* 83(2):587–645.
31. Candelier R, Dauchot O, Biroli G (2010) Dynamical facilitation decreases when approaching the granular glass transition. *EPL* 92(2):24003.
32. Biroli G, Garrahan JP (2013) Perspective: The glass transition. *J Chem Phys* 138(12):12A301.
33. Mishra CK, Rangarajan A, Ganapathy R (2013) Two-step glass transition induced by attractive interactions in quasi-two-dimensional suspensions of ellipsoidal particles. *Phys Rev Lett* 110(18):188301.
34. Elmatad YS, Keys AS (2012) Manifestations of dynamical facilitation in glassy materials. *Phys Rev E Stat Nonlin Soft Matter Phys* 85(6):061502.
35. Asakura S, Oosawa F (1954) On interaction between two bodies immersed in a solution of macromolecules. *J Chem Phys* 22(7):1255–1256.
36. Schiller P, Kruger S, Wahab M, Mogel HJ (2011) Interactions between spheroidal colloidal particles. *Langmuir* 27(17):10429–10437.
37. Gebremichael Y, Vogel M, Glotzer S (2004) Particle dynamics and the development of string-like motion in a simulated monoatomic supercooled liquid. *J Chem Phys* 120(9):4415–4427.
38. Schilling R, Scheidsteiger T (1997) Mode coupling approach to the ideal glass transition of molecular liquids: Linear molecules. *Phys Rev E Stat Phys Plasmas Fluids Relat Interdiscip Topics* 56(3):2932–2949.
39. Franosch T, Fuchs M, Götze W, Mayr MR, Singh A (1997) Theory for the reorientational dynamics in glass-forming liquids. *Phys Rev E Stat Phys Plasmas Fluids Relat Interdiscip Topics* 56(5):5659–5674.
40. Letz M, Schilling R, Latz A (2000) Ideal glass transitions for hard ellipsoids. *Phys Rev E Stat Phys Plasmas Fluids Relat Interdiscip Topics* 62(4):5173–5178.
41. De Michele C, Schilling R, Sciortino F (2007) Dynamics of uniaxial hard ellipsoids. *Phys Rev Lett* 98(26):265702.
42. Zheng Z, Wang F, Han Y (2011) Glass transitions in quasi-two-dimensional suspensions of colloidal ellipsoids. *Phys Rev Lett* 107(6):065702.
43. Zheng Z, et al. (2014) Structural signatures of dynamic heterogeneities in monolayers of colloidal ellipsoids. *Nat Commun* 5:3829.
44. Ho C, Keller A, Odell J, Ottewill R (1993) Preparation of monodisperse ellipsoidal polystyrene particles. *Colloid Polym Sci* 271(5):469–479.
45. Crocker JC, Grier DG (1996) Methods of digital video microscopy for colloidal studies. *J Colloid Interface Sci* 179(1):298–310.